
Improving Prototypical Part Networks with Reward Reweighing, Reselection, and Retraining

Robin Netzorg* Jiaxun Li* Bin Yu

University of California, Berkeley
* Equal Contribution

Abstract

In recent years, work has gone into developing deep interpretable methods for image classification that clearly attributes a model’s output to specific features of the data. One such of these methods is the *prototypical part network* (ProtoPNet), which attempts to classify images based on meaningful parts of the input. While this method results in interpretable classifications, it often learns to classify from spurious or inconsistent parts of the image. Hoping to remedy this, we take inspiration from the recent developments in Reinforcement Learning with Human Feedback (RLHF) to fine-tune these prototypes. By collecting human annotations of prototypes quality via a 1-5 scale on the CUB-200-2011 dataset, we construct a reward model that learns to identify non-spurious prototypes. In place of a full RL update, we propose the *reweighed, reselected, and retrained prototypical part network* (R3-ProtoPNet), which adds an additional three steps to the ProtoPNet training loop. The first two steps are reward-based reweighing and reselection, which align prototypes with human feedback. The final step is retraining to realign the model’s features with the updated prototypes. We find that R3-ProtoPNet improves the overall consistency and meaningfulness of the prototypes, but lower the test predictive accuracy when used independently. When multiple trained R3-ProtoPNets are incorporated into an ensemble, we find an increase in test predictive performance while maintaining interpretability.

1 Introduction

With the widespread use of deep learning, having these models be interpretable is more important now than ever. As these models continue to see use in high-stakes situations, practitioners hoping to justify a decision need to understand how a deep model makes a prediction, and trust that those explanations are valuable and correct [15]. One such proposed method for image classification is the *prototypical part network* (ProtoPNet), which classifies a given image based on its similarity to prototypical parts of training images, called prototypes [7]. This model aims to combine the power of deep learning with an intuitive reasoning module similar to humans.

While ProtoPNet aims to learn meaningful prototypical concepts, in practice, learned prototypes suffer from learning spurious concepts, such as the background of an image, from inconsistent concepts, such as learning both the head and the wing of a bird, and from duplicating concepts, such as having two prototypes that correspond to the same wing of the same bird [5]. Such problems are highly detrimental to the efficacy of these models, resulting in wasted computation at best and incorrect reasoning at worst. Various methods have been proposed to account for these issues [5, 13, 4], but these methods involve either costly labelling procedures or fall short of providing a means of measuring prototype quality.

We seek to increase the performance of the learned prototypes by taking inspiration from recent advances in reinforcement learning with human feedback (RLHF) [14] and reward learning [12]. RLHF and reward learning have become popular approaches for aligning large language models with human preferences, partially due to the flexibility of learned rewards and feedback collection methods [2]. While prior work has incorporated human feedback into ProtoPNETs [4, 5], no variation of ProtoPNET has incorporated a cheap and flexible reward learning fine-tuning framework.

Towards this end, we propose the *reward reweighed, reselected, and retrained prototypical part network* (R3-ProtoPNET), which seeks to improve the original ProtoPNET via fine-tuning with a learned reward model. With minimal human feedback data on the Caltech-UCSD Birds-200-2011 (CUB-200-211) dataset [20], we are able to train a high-quality reward model that achieves 91.5% test accuracy when ranking human preferences, serving as a strong measure for prototype quality. R3-ProtoPNET is then able to improve the meaningfulness of prototypes, removing dependence on spurious features, and is able to slightly decrease inconsistency across images compared to the original ProtoPNET. When used as base learners in an ensemble, R3-ProtoPNET is able to outperform an ensemble of ProtoPNETs on a held-out test dataset.

In summary, our contributions are as follows. Firstly, we demonstrate that a reward model trained on small amounts of human feedback data (roughly 300 ratings) can accurately rank human preference data. Secondly, due to the high performance of the reward model, we propose using the reward model as a measure of prototype. Thirdly, we introduce the R3-ProtoPNET, which uses reward-guided fine-tuning to improve prototype meaningfulness and ensemble performance.

2 Related Work

2.1 Reinforcement Learning with Human Feedback

Since the success of InstructGPT [14], Reinforcement Learning with Human Feedback (RLHF) has received a great deal of attention in the machine learning community. Although this success is recent, incorporating human feedback into reinforcement learning methods via a learned reward model has a deep history in reward learning [8, 11]. While works taking inspiration from InstructGPT have used proximal policy optimization (PPO) to fine-tune networks with human feedback [3], it is unclear to the extent that formal reinforcement learning is necessary to improve models via learned reward functions [12], or if the human feedback needs to follow a particular form [2]. Some prior work incorporates the reward function as a way to weigh the likelihood term [17, 22]. Keeping this work in mind, we incorporate the reward model into ProtoPNET as a way to reweigh prototypes post-training.

2.2 Example-based Models and Prototypical Part Networks

The field of interpretable deep learning is vast, with a plethora of explainability and interpretability methods available to the user. For a more complete overview of interpretable deep learning, please refer to Rudin et al. [15]. To ground the discussion, we focus primarily on example-based models, one such example being ProtoPNET. While ProtoPNET is our model of interest, other example-based methods exist, such as the non-parametric xDNN [1] or SITE, which performs predictions directly from interpretable prototypes [19]. While other example-based methods exist, we focus on the ProtoPNET due to its intuitive reasoning structure.

Since its introduction by Chen et al. [7], ProtoPNETs have received a great deal of attention, and various iterations have been developed. Work has explored extending the ProtoPNET to different architectures such as transformers ([21]), or sharing class information between prototypes ([16]). Donnelly et al. [9] increase the spatial flexibility of ProtoPNET, allowing prototypes to change spatial positions depending on the pose information available in the image. ProtoPNETs and variations have seen success in high-stakes applications, such as kidney stone identification ([10]) and mammography ([4]).

Many works have commented on how the original ProtoPNET tends to overemphasize spurious features, and they have taken different approaches to solving this issue. Nauta et al. [13] introduce an explainability interface to ProtoPNET, allowing users to see the dependence of the prototype on certain image attributes like hue and shape. The authors claim that seemingly dissimilar or spurious prototypes share certain difficult-to-perceive features, like texture or contrast. Barnett et al. [4]

introduce a variation of the ProtoPNet, IAIA-BL, which biases prototypes towards expert labelled annotations of classification-relevant parts of the image.

Similar to how we provide human feedback at the interpretation level, Bontempelli et al. [5] introduce the ProtoPDebug, where a user labels a prototype and image pair as "forbidden" or "valid", and a fine-tuning step maximizes the distance between learned prototypes and patches in the forbidden set and minimizes the distance between learned prototypes and patches in the valid set. While also incorporating human feedback, [5] do not ground their method in RLHF, but instead includes the binary feedback as a supervised constraint into the ProtoPNet loss function. Learning a reward function via ratings allows us to simultaneously increase the interpretability of the prototypes, and develop an evaluation metric for the quality of a particular prototype. Compared to previous approaches, reward reweighing, reselection, and retraining allows for fast collection of high-quality human feedback data and the construction of a reward model that measures prototype quality while increasing the interpretability and the performance of the model.

3 Prototypical Part Network (ProtoPNet)

In this section, we describe the base architecture used in our method, the Prototypical Part Network (ProtoPNet) introduced in Chen et al. [7]. The ProtoPNet aims to introduce interpretability to otherwise uninterpretable image classifiers. In place of predicting from an arbitrary representation, the model makes a classification based on part attention and similar prototypical parts of an image. The general reasoning of a model is to classify an unseen image by finding training images with similar prototypical parts to those of the unseen image. This approach allows the user to interrogate the reasoning of the model, and clearly see which parts of the image led to the model’s classification.

3.1 Description

Here we briefly describe the ProtoPNet, adopting the notation used in Chen et al. [7]. The ProtoPNet architecture builds on a base convolutional neural network f , which is then followed by a prototype layer denoted g_p , and a fully connected layer h . Typically, the convolutional features are taken pretrained models like VGG-19, ResNet-34, or DenseNet-121.

The ProtoPNet injects interpretability into these convolutional architectures with the prototype layer g_p , consisting of m prototypes $\mathbf{P} = \{p_j\}_{j=1}^m$ typically of size $1 \times 1 \times D$, where D is the shape of the convolutional output $f(x)$. By keeping the depth the same as the output of the convolutional layer, but restricting the height and width to be smaller than that of the convolutional output, the learned prototypes select a patch of the convolutional output. Reversing the convolution leads to recovering a prototypical patch of the original input image x . Using upsampling, the method constructs a activation pattern per prototype p_j .

To use the prototypes to make a classification given a convolutional output $z = f(x)$, ProtoPNet’s prototype layer computes a max pooling over similarity scores: $g_{p_j}(z) = \max_{\tilde{z} \in \text{patches}(z)} \log((\|\tilde{z} - p_j\|_2^2 + 1)(\|\tilde{z} - p_j\|_2^2 + \epsilon))$, for some small $\epsilon < 1$. This function is monotonically decreasing with respect to the distance, with small values of $\|\tilde{z} - p_j\|_2^2$ resulting in a large similarity score $g_{p_j}(z)$. Assigning m_k prototypes for all K classes, such that $\sum_{k=1}^K m_k = m$, the prototype layer outputs a vector of similarity scores that matches parts of the latent representation z to prototypical patches across all classes. The final layer in the model is a linear layer connecting similarities to class predictions.

In order to ensure that the prototypes match specific parts of training images, during training the prototype vectors are projected onto the closest patch in the training set. For the final trained ProtoPNet, every p_j corresponds to some patch of a particular image.

3.2 Limitations

While ProtoPNet is capable of providing interpretable classifications, the base training described in Chen et al. [7] results in prototypes that are inconsistent and represent spurious features of the image ([4, 5]). Additionally, same-class prototypes will often converge to the same part of the image, resulting in duplicate prototypes.

Chen et al. [7] note that a prototype whose top L (usually $L = 5$) closest training image patches come from different classes than the target class tend to be spurious and inconsistent, focusing on features like the background. To remedy this issue, they introduce a pruning operation, removing these prototypes entirely. While pruning does remove dependency on some subpar prototypes, we find that pruning still leaves some prototypes that rely on spurious and inconsistent features (Table 3) and does not improve accuracy. We also find that duplicate prototypes still occur after the pruning operation as well. We visualize subpar prototypes in Figure 1. For more examples of low-quality prototypes, please see the supplementary material.

4 Human Feedback and the Reward Reweighed, Reselected, and Retrained Prototypical Part Network (R3-ProtoPNet)

Inspired by the recent advances in reinforcement learning with human feedback (RLHF) [14], the reward reweighed, reselected, and retrained prototypical part network (R3-ProtoPNet) utilizes a learned reward model to fine-tune prototypes. In place of pruning prototypes and sacrificing potential information, we demonstrate that incorporating human feedback into the training of the ProtoPNet improves prototype quality while increasing ensemble accuracy. In this section, we describe the collection of high-quality human feedback data, our reward model, and how we incorporate the reward model into the training loop via a three-stage training procedure.

4.1 Human Feedback Collection

A crucial aspect behind the success of RLHF methods is the collection of high quality human feedback data. Unclear or homogeneous feedback may result in a poor performing reward model [8]. The design of human feedback collection is vitally important to the training of a useful reward model.

The inherent interpretability of ProtoPNet leads to a useful benefit for RLHF. Given a trained ProtoPNet, it is possible for a knowledgeable user to directly critique the learned prototypes. Given a particular classification task, a human with enough expertise should be able to recognize if a particular prototype is "good" or "bad" [5]. In the case of classifying birds in the CUB-200-2011 dataset, one of the original classification tasks used in Chen et al. [7], it is clear that if a prototype gives too much weight to the background of the image (spurious), or if the prototype corresponds to different parts of the bird when looking at different images (inconsistency), the learned prototype is not meaningfully or interpretably contributing to prediction. Given these prototypes that fail to contribute to prediction, a knowledgeable human trying to classify birds would rate these prototypes as "bad".

There are many different ways to elicit this notion of "goodness" from a user [2]. Although it is possible to incorporate many different forms of feedback into the R3-ProtoPNet, such as asking a user to compare prototypes to elicit preferences or ask for a binary value of whether a prototype is "good" or "bad", we found most success with asking the user to rate a prototype on a scale from 1 to 5. While scalar ratings can be unstable across different raters, with a clear, rule-based rating method, rating variance is reduced and it is possible to generate high-quality labels. An example rating scale on the CUB-200-2011 dataset is provided in Figure 1.

4.2 Reward Learning

We note that, when a user provides feedback on a prototype, it is not the training image or the model prediction that the user is providing feedback on, but the prototype's resulting interpretation: the activation patterns. Our task is therefore different from RLHF applied to language modeling or RL tasks ([14], [8]), where human feedback is provided on the model output or resulting state. We therefore collect a rating dataset $\mathcal{D} = \{(x_i, y_i, h_{i,j}, r_{i,j})\}_{i=1, j=1}^{n,m}$, where x_i, y_i are the training image and label, and $h_{i,j}, r_{i,j}$ are prototype p_j 's activation patterns and user-provided activation patterns for image x_i . We note that collecting preferences for this entire dataset is prohibitive and unnecessary, so we only collect a subset.

Given the dataset \mathcal{D} , we generate the induced comparison dataset, whereby each entry in \mathcal{D} is paired with one another. Given $i \neq i'$ and/or $j \neq j'$, we populate a new paired dataset, \mathcal{D}_{paired} , which consists of the entries of \mathcal{D} indexed by i, j, i', j' , and a comparison c , which takes values $-1, 0, 1$. If the left-hand sample is greater, and therefore considered higher-quality, $r_{i,j} > r_{i',j'}$, then $c = -1$. If

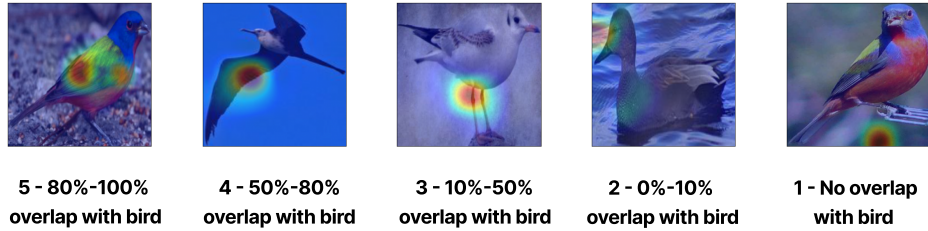


Figure 1: Rubric used for human feedback on the activation patterns of predictions for birds from the CUB-200-2011 dataset. Ratings of 4-5 are correspond to high-quality prototypes, 1-2 to low-quality prototypes, and 3 to unclear quality prototypes.

the right-hand sample is greater $r_{i,j} < r_{i',j'}$, then $c = 1$. We note that, during learning, we exclude entries with $c = 0$ to increase the contrast between pairs. This synthetic construction allows us to model the reward function, $r(x_i, h_{i,j})$, via the Bradley-Terry Model for pairwise preferences [6]. We train this model with the same loss function as in Christiano et al. [8], a cross-entropy loss over the probabilities of ranking one pair over the other. This synthetic construction combinatorially increases the amount of preference data, allowing us to train a high-quality reward model on relatively small amounts of quality human feedback data.

4.3 Reward Reweighed, Reselected, and Retrained Prototypical Part Network (R3-ProtoPNet)

After having collected high-quality human feedback data and trained a reward model, we can now incorporate it into a fine-tuning framework to improve the interpretability of ProtoPNet. We incorporate the reward model via a three step process consisting of reward weighting, reselection, and retraining. Each step is described in more detail below.

4.3.1 Reward Reweighting

Although PPO is a popular option for RLHF ([14]), there is evidence that simpler fine-tuning algorithms can lead to similar performance increases ([2]). Inspired by the success and the ease of implementation of reward-weighted learning [12, 17, 22], we develop a reward-weighted update for the ProtoPNet:

$$\max_{p_j} \mathcal{L}_{reweigh}(z_i^*, p_j) = \max_{p_j} \sum_{i \in I(p_j)} r(x_i, p_j) \frac{1}{\lambda_{dist} \|z_i^* - p_j\|_2^2 + 1} \quad (1)$$

where $z_i^* = \operatorname{argmin}_{z \in \text{patches}(f(x_i))} \|z - p_j\|_2^2$, $I(p_j) = \{i \mid y_i \in \text{class}(p_j)\}$, and λ_{dist} is a fixed hyperparameter. We note that the loss function \mathcal{L}_{reg} is a sum of the inverse distances weighted by the reward of the prototype on that image. Since we only update the prototype p_j , the only way to maximize the loss is to minimize the distance between prototype and image patches with high reward $r(x_i, p_j)$. This causes the prototype to resemble high reward image patches, improving the overall quality of the prototypes. Wanting to preserve prototypes that already have high reward, we only update those prototypes that have relatively low mean reward less than $\gamma = 0.45$. λ_{dist} is included in the loss function to rescale distances, since the closest distances are near zero. We find best performance with $\lambda_{dist} = 100$.

Practically, we find that optimizing this loss function leads to locally maximal solutions, resulting in local updates that do not modify prototypes with low quality values of 1, but it's more likely to improve prototypes with quality values of 2 or higher. If the prototype p_j has high activation over the background of an image x_i , for example, the closest patches z_i^* in the training data will also be background patches, and the reward of the prototype will be low, leaving minimal room for change.

It is not possible for this update to dramatically change the location of the patch in the image via this loss function.

4.3.2 Prototype Reselection

In order to improve low quality prototypes that require significant manipulation, we introduce a reselection procedure based on a reward threshold. Given a prototype p_j and image x_i , if $\frac{1}{n_k} \sum_{i \in I(p_j)} r(x_i, p_j) < \alpha$, where α is a pre-determined threshold and n_k is the number of training images in class k , we reselect the prototype. The reselection process involves iterating over patch candidates z'_i and temporarily setting the prototype $p'_j = z'_i$, where z'_i is chosen randomly from the patches of a randomly selected image x'_i in the class of p_j . If $\frac{1}{n_k} \sum_{i \in I(p_j)} r(x'_i, p'_j) > \beta$, where β is an acceptance threshold, and if none of the prototypes match patch $p'_j = z'_i$, then we accept the patch candidate as the new prototype. We found that $\alpha = 0.15$ and $\beta = 0.50$ led to good performance. We refer to the combination of reweighting and reselection as the R2 update step, and the corresponding trained model the R2-ProtoPNet.

The reasoning process behind our prototype reselection method takes inspiration from the original push operation in Chen et al. [7]. Similar to how ProtoPNet projects prototypes onto a specific training image patch, here we reselect prototypes to be a particular reward-filtered training image patch. With a high enough acceptance threshold β , this forces the elimination of low reward prototypes while preserving the information gain of having an additional prototype.

One possible alternative approach is to instead search over the training patches, and select those patches with the highest reward. We found that randomly selecting patches, in place of searching for patches with the highest reward, led to higher prototype diversity and less computation time. As discussed in Section 6, it is possible that a reward model that more explicitly accounts for prototype diversity could alleviate the duplicate issue, but we leave this to future work.

While we do not use a traditional reinforcement learning algorithm to fine-tune our model as is typically done in RLHF [2], pairing the reselection and fine-tuning steps together resembles the typical explore-exploit trade-off in RL problems. We see that fine-tuning with our reward model leads to exploit behavior, improving upon already high-quality prototypes. At the same time, the reselection step serves as a form of exploration, drastically increasing the quality of uninformative prototypes. We find that these similarities are enough to improve the quality of ProtoPNet, as discussed in the next section.

4.3.3 Retraining

A critical step missing in the R2 update is a connection to prediction accuracy. As discussed in Section 5, without incorporating predictive information, performing the reward update alone results in lowered test accuracy. Since the above updates only act on the prototypes themselves, not the rest of the network, the result is a misalignment between the prototypes and the model’s base features and final predictive layer. The reward update guides the model towards more interpretable prototypes, but the reward update alone fails to use the higher quality prototypes for better prediction.

To account for the lack of predictive performance, the final step of R3-ProtoPNet is retraining. Simply retraining with the same loss function used in the original ProtoPNet update results in the realignment of the prototypes and the rest of the model. Although one could worry that predictive accuracy would reduce the interpretability of the model [15], we find that retraining increases predictive accuracy while maintaining the quality increases of the R2 update. The result is a high accuracy model with higher-quality prototypes. We explore evidence of this phenomenon and why this is the case in the following section.

5 Experiments

Here we discuss the results of training the R3-ProtoPNet on the CUB-200-2011 dataset, the same dataset as used in Chen et al. [7]. We demonstrate that the R3-ProtoPNet leads for higher quality prototypes across base model architectures and prototype configurations while not sacrificing predictive performance.

5.1 Datasets

R3-ProtoPNet requires two datasets: the original dataset for initial training, and the scalar ratings of activation pattern dataset. Combined, this results in the dataset described in Section 4. To offer better comparison against the original ProtoPNet, we use the same dataset for initial training that was used in Chen et al. [7], the CUB-200-2011 dataset [18]. The CUB-200-2011 dataset consists of roughly 30 images of 200 different bird species. We employ the same data augmentation scheme used in Chen et al. [7], which adds additional training data by applying a collection of rotation, shear, and skew perturbations to the images, resulting in a larger augmented dataset.

For the collection of the activation pattern ratings, we only provide activation patterns overlaid on the original images to the rater. Although it is possible to crowdsource the collection of human preference data, we found that it was possible to increase the performance of ProtoPNet with relatively small amounts human preference data that we ourselves collected. We rated a total of 700 prototype-image pairs according to the scale approach described in Figure 1, which we justify in the next subsection.

5.2 Architectures and Training

Similar to Chen et al. [7], we study the performance of R3-ProtoPNet across three different base architectures: VGG-19, ResNet-34, and DenseNet-121. While the original ProtoPNet sets the number of prototypes per class at $m_k = 10$, we additionally run the VGG19 architecture with $m_k = 5$ prototypes to explore model performance when the number of prototypes is limited. No other modifications were made to the original ProtoPNet architecture. We train for 100 epochs and report results for the best performing model.

The reward model $r(x_i, h_i)$ is similar to the base architecture of the ProtoPNet. Two ResNet-50 base architectures take in the input image x_i and the associated activation pattern h_i separately, and both have two additional convolutional layers. The outputs of the convolutional layers are concatenated and fed into a final linear layer with sigmoid activation to predict the Bradley-Terry ranking. Predicted rewards are therefore bound in the range $(0, 1)$. We train the reward model for 5 epochs on a comparison dataset of 71,875 paired images and preference labels, and evaluate on a 13,831 testing pairs. The reward model achieves 91.54% test accuracy when trained on the whole dataset, and we additionally find that the reward model converges to roughly 91% test accuracy on a comparison dataset generated from at least 300 rated activation patterns.

5.3 Evaluation Metrics

To evaluate the performance of R3-ProtoPNet, we compare it to ProtoPNet using three metrics: test accuracy, reward, and prototype class mismatch. We use test accuracy to measure the predictive performance of the models. As the above section demonstrates, the learned reward model achieves high accuracy in predicting which prototype ranks above another in accordance with human preferences, so we therefore use it as a measure of prototype quality. Regarding the class mismatch metric, Chen et al. [7] note that low-quality prototypes tend to have close training images that come from different classes. To evaluate the effect of R3 updating, we compute the average class mismatch across all prototypes for a given model for the Top-5 and Top-10 closest training images.

5.4 Results

After training ProtoPNet, running the R2 update step, and then performing retraining, we see several trends across multiple base architectures. In Table 1, we report the test accuracy of the different base architectures across stages of R3-ProtoPNet training. Generally, the test accuracy from ProtoPNet substantially decreases after applying the R2 update, but retraining tends to recover most of the predictive loss. This accuracy maintenance demonstrates that it is possible to align prototypes with human preferences without sacrificing predictive power.

In Table 2, we report the average reward of all prototypes on all test images for a given base architecture. We see that ProtoPNet achieves an average reward between 0.48 and 0.57 across architectures. Investigating the distribution of rewards further in Figure 2a, it is revealed that ProtoPNet tends to produce a bimodal distribution over prototype rewards, with some bias towards low-quality and high-quality prototypes. Applying the R2 update results in the desired behavior, increasing the average reward and shifting the distribution of rewards upwards. We additionally see

Base (m_k)	ProtoPNet	R2-ProtoPNet	R3-ProtoPNet
VGG-19 (5)	73.44%	57.36%	74.12%
VGG-19 (10)	73.80%	54.25%	74.73%
ResNet-34 (10)	77.49%	52.88%	76.32%
DenseNet-121 (10)	75.68%	64.18%	74.63%
Ensemble (VGG-19(10) + ResNet-34 + DenseNet-121)	80.53%	74.89%	80.86%
Ensemble (All 4 Base Models)	80.91%	77.77%	82.00%

Table 1: Test accuracy of different base architectures during the stages of R3-ProtoPNet training, where m_k is the number of prototypes per class. Ensembles consist of the corresponding individually trained networks.

Base (m_k)	ProtoPNet	R2-ProtoPNet	R3-ProtoPNet
VGG19 (5)	0.56	0.64	0.68
VGG19 (10)	0.48	0.65	0.65
ResNet34 (10)	0.57	0.61	0.65
DenseNet121 (10)	0.52	0.68	0.69

Table 2: Average rewards over the test dataset of different base architectures during the stages of R3-ProtoPNet training.

that the retraining step in R3-ProtoPNet actually continues to increase average reward across all base architectures while slightly increasing the spread of the reward distribution.

Finally, we report the Top-5 and Top-10 class mismatch in Table 3. Here we see an interesting phenomena. Across all base architectures, ProtoPNet has an average class mismatch of at least half of the Top-L closest image patches, for both $L = 5, 10$. Although performing the R2 greatly increases the average reward for all base architectures except ResNet-34, we see that class mismatch is only marginally reduced, with still all of the base architectures resulting in mismatches for over half of the closest Top-L training image patches. We see that R3-ProtoPNet greatly reduces class mismatch for the $m_k = 5$ VGG-19 base architecture, but tends to only marginally reduce class mismatch for the $m_k = 10$ case.

5.5 Discussion

Given the results, we see that R3-ProtoPNet manages to increase the quality of learned prototypes without sacrificing predictive performance. While the ResNet-34 and DenseNet-121 base architectures do see a slight performance decrease, producing an ensemble of trained R3-ProtoPNets results in an accuracy increase over an ensemble of the original trained ProtoPNets. We see that R3-ProtoPNet results in a substantial increase of the average test reward, verifying that prototype quality is increasing. There is still much room for improvement, as class mismatch for 10 prototypes does not decrease across all architectures, while there is some class mismatch decrease for the 5 prototype VGG-19-based ProtoPNet. Overall, these results demonstrate that incorporating reward information into the ProtoPNet via reweighing, reselection, and retraining does increase interpretability of ProtoPNets, and, when incorporated into an ensemble, increases predictive performance.

Base (m_k)	ProtoPNet	R2-ProtoPNet	R3-ProtoPNet
VGG19 (5)	2.77, 5.75	2.59, 5.39	1.45, 3.16
VGG19 (10)	3.28, 6.82	3.00, 6.30	2.77, 5.84
ResNet34 (10)	4.07, 8.52	4.05, 8.37	4.05, 8.29
DenseNet121 (10)	3.52, 7.49	2.78, 6.26	3.55, 6.53

Table 3: Average class mismatch of prototypes and the Top-5, Top-10 closest training image patches across different base architectures during the stages of R3-ProtoPNet training.

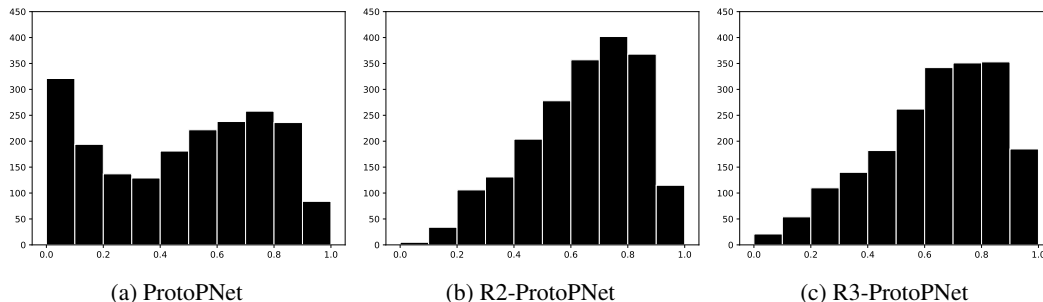


Figure 2: Histograms of the rewards of prototype,image pairs for (a) ProtoPNet, (b) R2-ProtoPNet, and (c) R3-ProtoPNet using VGG19 with 10 prototypes per class.

6 Limitations and Future Work

While R3-ProtoPNet improves interpretability and predictiveness in an ensemble, there is plenty of room for improvement. We note that the reward model is trained on ratings of a single image and heatmap, highly constrained to measuring overlap between prototype and the object of interest, but it is quite possible to extend ratings to multiple images and heatmaps. This would allow for the reward model to better learn cross-image preferences, such as consistency. We hope that this could alleviate the duplicate issue as well. We note that R3-ProtoPNet fails to entirely eliminate duplicates, with several high-reward prototypes converge to the same part of the image.

While this work investigated increasing the performance of ProtoPNet, it is possible to extend the R3 update to other extensions of the ProtoPNet. A major benefit of reward fine-tuning is its flexibility in application, and we expect that combining the R3 update with other variations of the ProtoPNet would result in further increased performance gains. Combining multiple feedback modalities, such as the binary feedback used in ProtoPDebug [5], could further increase model performance.

A final limitation with R3-ProtoPNet and other methods that rely on human feedback is that the model itself might be learning features that, while seemingly confusing to a human, are helpful and meaningful for prediction. Barnett et al. [4] argue that the ProtoPNet can predict with non-obvious textures like texture and contrast, which might be penalized via a learned reward function. Future work is necessary to investigate how ProtoPNet variants could critique human feedback, and argue against a learned reward function.

7 Conclusion

In this work, we propose the R3-ProtoPNet, a method that uses a learned reward model of human feedback to improve the meaningfulness of learned prototypical parts. We find that ensembling multiple R3-ProtoPNets results in increased performance over original ProtoPNet ensembles. Considering the high performance of the reward model, we use the reward model as a measure of prototype quality, allowing us to critique the interpretability of ProtoPNet along a human lens. The ability of reward learning to quantize qualitative human preferences make reward-based fine-tuning a promising direction for the improvement of interpretable deep models.

References

- [1] P. Angelov and E. Soares. Towards explainable deep neural networks (xdnn), 2019.
- [2] A. Askeell, Y. Bai, A. Chen, D. Drain, D. Ganguli, T. Henighan, A. Jones, N. Joseph, B. Mann, N. DasSarma, et al. A general language assistant as a laboratory for alignment. *arXiv preprint arXiv:2112.00861*, 2021.
- [3] Y. Bai, A. Jones, K. Ndousse, A. Askeell, A. Chen, N. DasSarma, D. Drain, S. Fort, D. Ganguli, T. Henighan, N. Joseph, S. Kadavath, J. Kernion, T. Conerly, S. El-Showk, N. Elhage, Z. Hatfield-Dodds, D. Hernandez, T. Hume, S. Johnston, S. Kravec, L. Lovitt, N. Nanda, C. Olsson,

- D. Amodei, T. Brown, J. Clark, S. McCandlish, C. Olah, B. Mann, and J. Kaplan. Training a helpful and harmless assistant with reinforcement learning from human feedback, 2022.
- [4] A. J. Barnett, F. R. Schwartz, C. Tao, C. Chen, Y. Ren, J. Y. Lo, and C. Rudin. Iaia-bl: A case-based interpretable deep learning model for classification of mass lesions in digital mammography, 2021.
- [5] A. Bontempelli, S. Teso, K. Tentori, F. Giunchiglia, and A. Passerini. Concept-level debugging of part-prototype networks, 2023.
- [6] R. A. Bradley and M. E. Terry. Rank analysis of incomplete block designs: I. the method of paired comparisons. *Biometrika*, 39(3/4):324–345, 1952.
- [7] C. Chen, O. Li, D. Tao, A. Barnett, C. Rudin, and J. K. Su. This looks like that: deep learning for interpretable image recognition. *Advances in neural information processing systems*, 32, 2019.
- [8] P. F. Christiano, J. Leike, T. Brown, M. Martic, S. Legg, and D. Amodei. Deep reinforcement learning from human preferences. *Advances in neural information processing systems*, 30, 2017.
- [9] J. Donnelly, A. J. Barnett, and C. Chen. Deformable protopnet: An interpretable image classifier using deformable prototypes. In *Proceedings of the IEEE/CVF Conference on Computer Vision and Pattern Recognition (CVPR)*, pages 10265–10275, June 2022.
- [10] D. Flores-Araiza, F. Lopez-Tiro, E. Villalvazo-Avila, J. El-Beze, J. Hubert, G. Ochoa-Ruiz, and C. Daul. Interpretable deep learning classifier by detection of prototypical parts on kidney stones images, 2022.
- [11] H. J. Jeon, S. Milli, and A. Dragan. Reward-rational (implicit) choice: A unifying formalism for reward learning. In H. Larochelle, M. Ranzato, R. Hadsell, M. Balcan, and H. Lin, editors, *Advances in Neural Information Processing Systems*, volume 33, pages 4415–4426. Curran Associates, Inc., 2020. URL https://proceedings.neurips.cc/paper_files/paper/2020/file/2f10c1578a0706e06b6d7db6f0b4a6af-Paper.pdf.
- [12] K. Lee, H. Liu, M. Ryu, O. Watkins, Y. Du, C. Boutilier, P. Abbeel, M. Ghavamzadeh, and S. S. Gu. Aligning text-to-image models using human feedback. *arXiv preprint arXiv:2302.12192*, 2023.
- [13] M. Nauta, A. Jutte, J. Provoost, and C. Seifert. This looks like that, because ... explaining prototypes for interpretable image recognition. In *Communications in Computer and Information Science*, pages 441–456. Springer International Publishing, 2021. doi: 10.1007/978-3-030-93736-2_34. URL https://doi.org/10.1007/978-3-030-93736-2_34.
- [14] L. Ouyang, J. Wu, X. Jiang, D. Almeida, C. L. Wainwright, P. Mishkin, C. Zhang, S. Agarwal, K. Slama, A. Ray, J. Schulman, J. Hilton, F. Kelton, L. Miller, M. Simens, A. Askell, P. Welinder, P. Christiano, J. Leike, and R. Lowe. Training language models to follow instructions with human feedback, 2022.
- [15] C. Rudin, C. Chen, Z. Chen, H. Huang, L. Semenova, and C. Zhong. Interpretable machine learning: Fundamental principles and 10 grand challenges, 2021.
- [16] D. Rymarczyk, L. Struski, J. Tabor, and B. Zieliński. Protopshare: Prototypical parts sharing for similarity discovery in interpretable image classification. In *Proceedings of the 27th ACM SIGKDD Conference on Knowledge Discovery & Data Mining, KDD '21*, page 1420–1430, New York, NY, USA, 2021. Association for Computing Machinery. ISBN 9781450383325. doi: 10.1145/3447548.3467245. URL <https://doi.org/10.1145/3447548.3467245>.
- [17] N. Stiennon, L. Ouyang, J. Wu, D. M. Ziegler, R. Lowe, C. Voss, A. Radford, D. Amodei, and P. Christiano. Learning to summarize from human feedback, 2022.
- [18] C. Wah, S. Branson, P. Welinder, P. Perona, and S. J. Belongie. The caltech-ucsd birds-200-2011 dataset. 2011.

- [19] Y. Wang and X. Wang. Self-interpretable model with transformationequivariant interpretation, 2021.
- [20] P. Welinder, S. Branson, T. Mita, C. Wah, F. Schroff, S. Belongie, and P. Perona. Caltech-ucsd birds 200. Technical Report CNS-TR-201, Caltech, 2010. URL [/se3/wp-content/uploads/2014/09/WelinderEtal10_CUB-200.pdf](#), <http://www.vision.caltech.edu/visipedia/CUB-200.html>.
- [21] M. Xue, Q. Huang, H. Zhang, L. Cheng, J. Song, M. Wu, and M. Song. Protopformer: Concentrating on prototypical parts in vision transformers for interpretable image recognition, 2022.
- [22] D. M. Ziegler, N. Stiennon, J. Wu, T. B. Brown, A. Radford, D. Amodei, P. Christiano, and G. Irving. Fine-tuning language models from human preferences. *arXiv preprint arXiv:1909.08593*, 2019.